

DOCUMENT CONTROL SHEET

	ORIGINATOR'S REF. NLR-TP-2004-149		SECURITY CLASS. Unclassified												
ORIGINATOR National Aerospace Laboratory NLR, Amsterdam, The Netherlands															
TITLE Two cryogenic NLR Balances for the ETW Twin Sting Rig															
PRESENTED AT at the Fourth International Symposium on Strain Gauge Balances, at San Diego - USA on 10-13 May 2004															
PERMISSION															
AUTHORS H.J. Alons and M.C.N. Wright* <small>*European Transonic Windtunnel GmbH</small>		DATE April 2004	<table border="1" style="width: 100%; border-collapse: collapse;"> <tr> <td style="width: 50%;">PP</td> <td style="width: 50%;">REF</td> </tr> <tr> <td style="text-align: center;">29</td> <td style="text-align: center;">5</td> </tr> </table>	PP	REF	29	5								
PP	REF														
29	5														
DESCRIPTORS <table style="width: 100%; border: none;"> <tr> <td style="width: 33%;">CALIBRATION</td> <td style="width: 33%;">AERODYNAMIC INTERFERENCE EFFECTS</td> <td style="width: 33%;">CRYOGENIC WIND TUNNEL</td> </tr> <tr> <td>DESIGN</td> <td>FINITE ELEMENT METHOD</td> <td>STING CORRECTIONS</td> </tr> <tr> <td>STRAIN GAUGE BALANCE</td> <td>STRAIN GAUGES</td> <td>TEST TECHNIQUES</td> </tr> <tr> <td>TWIN STING SUPPORT</td> <td>WIND TUNNEL MEASUREMENTS</td> <td></td> </tr> </table>				CALIBRATION	AERODYNAMIC INTERFERENCE EFFECTS	CRYOGENIC WIND TUNNEL	DESIGN	FINITE ELEMENT METHOD	STING CORRECTIONS	STRAIN GAUGE BALANCE	STRAIN GAUGES	TEST TECHNIQUES	TWIN STING SUPPORT	WIND TUNNEL MEASUREMENTS	
CALIBRATION	AERODYNAMIC INTERFERENCE EFFECTS	CRYOGENIC WIND TUNNEL													
DESIGN	FINITE ELEMENT METHOD	STING CORRECTIONS													
STRAIN GAUGE BALANCE	STRAIN GAUGES	TEST TECHNIQUES													
TWIN STING SUPPORT	WIND TUNNEL MEASUREMENTS														
ABSTRACT The existing Twin Sting Rig of the European Transonic Windtunnel had to be supplemented with two high accuracy cryogenic balances for the sting interference part of the HiReTT programme. NLR designed and manufactured these balances. Extensive use of the Finite Element Method was made during the design iterations. Dead weight single loads calibrations at NLR and calibrations of the complete load range at 12 different temperatures in the range of 325 to 115 K in the calibration machine of ETW, demonstrated that the achieved accuracy of each balance was within 0.1%. Dead weight loading of a dummy wing in the assembled Twin Sting Rig proved the concept of the Twin Sting Rig with two balances in the booms. The general level of uncertainty demonstrated during the subsequent HiReTT programme in the cryogenic European Transonic Windtunnel was better than 1 drag count.															



NLR-TP-2004-149

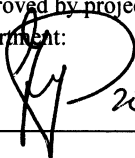
Two cryogenic NLR Balances for the ETW Twin Sting Rig

H.J. Alons and M.C.N. Wright*

**European Transonic Windtunnel GmbH

This report has been based on a paper to be presented at the Fourth International Symposium on Strain Gauge Balances, at San Diego – USA on 10-13 May 2004. This report may be cited on condition that full credit is given to NLR and the authors.

Customer: National Aerospace Laboratory NLR
Working Plan number: 1.1.I.1n/A.1.A.4
Owner: National Aerospace Laboratory NLR
Division: Aerospace Vehicles
Distribution: Unlimited
Classification title: Unclassified
April 2004

Approved by author:  280404	Approved by project manager:  280404	Approved by project managing department:  28/4/04
---	--	---



Summary

The existing Twin Sting Rig of the European Transonic Windtunnel had to be supplemented with two high accuracy cryogenic balances for the sting interference part of the HiReTT programme. NLR designed and manufactured these balances. Extensive use of the Finite Element Method was made during the design iterations. Dead weight single loads calibrations at NLR and calibrations of the complete load range at 12 different temperatures in the range of 325 to 115 K in the calibration machine of ETW, demonstrated that the achieved accuracy of each balance was within 0.1%. Dead weight loading of a dummy wing in the assembled Twin Sting Rig proved the concept of the Twin Sting Rig with two balances in the booms. The general level of uncertainty demonstrated during the subsequent HiReTT programme in the cryogenic European Transonic Windtunnel was better than 1 drag count.



Contents

1	Introduction	5
2	Design	6
2.1	Specification	6
2.2	Balance design	8
2.3	Additional parts	16
3	Manufacturing	16
4	Checks	17
5	Calibration Activities	17
5.1	Ambient dead weight loading calibration at NLR	17
5.2	Calibration at ETW in the Balance Calibration Machine	18
5.3	Check Loadings on Individual Balances	21
5.4	Connected Balance Check Loadings	22
6	Twin Sting Rig Wind Tunnel Test Results	24
7	Conclusions	29
8	References	29

(29 pages in total)



1 Introduction

Since 1998 the European Transonic Windtunnel (ETW) has a Twin Sting Rig (TSR) available for cryogenic wind tunnel tests. The TSR enables full span models to be tested such that the localized effects of the rear sting support interference can be obtained by measuring the loads and pressures acting on the rear fuselage with and without a dummy rear sting, see Figure 1.

The TSR was designed and manufactured by NLR and contained two simple 3 component balances or so-called 'flexures' in both booms. These flexures are mainly intended as load monitoring devices and can be used in combination with a separate after body balance mounted in the split rear fuselage in order to derive the sting interference effects. This form of the TSR technique is referred to as the 'standard' method.

The collaborative research project HiReTT (High Reynolds Number Tools and Techniques for Civil Aircraft Design) is focused on understanding the effects of scale on aircraft performance and establishing the capability to account for these effects within the design process.



Figure 1: High speed generic cryogenic model installed on the ETW Twin Sting Rig

The project, formed by a consortium of industry and research centres, including NLR and ETW, was launched in January 2000 as part of the Key Action Aeronautics within the Fifth Research Framework Programme of the European Union. For this project it was necessary to develop the 'enhanced' TSR. In some aircraft models there is not enough space available for an afterbody balance or for instrumentation cable routing through the wing. In that case the 'enhanced' TSR is more appropriate. In the enhanced method forces acting on the complete model with and without a dummy central rear sting are measured using two high accuracy 6-component balances in the TSR booms. The location of the balances in the TSR is shown in Figure 2. In close co-operation with ETW, NLR has designed and manufactured these two cryogenic balances. This paper describes the design, manufacturing and calibration of the balances. Also

the check loadings of the connected balances and some of the experiences with the enhanced TSR in the cryogenic ETW wind tunnel are presented. The ‘standard’ and ‘enhanced’ TSR test techniques itself are more thoroughly presented in Reference 1.

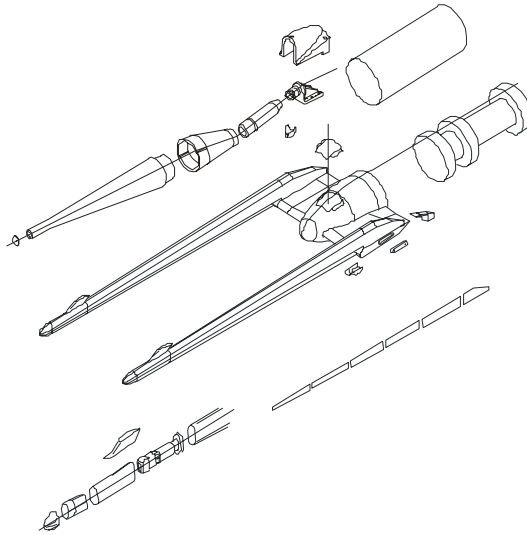


Figure 2: Exploded view of the TSR including balances

2 Design

2.1 Specification

The main requirements set for the two identical balances were:

- same interfaces as the existing flexures,
- total length may increase from 300 mm (flexures) to 400 mm (balances),
- through-balance wiring of 40 wires AWG36 and 2 pneumatic tubes,
- static combined aerodynamic model loads according Table 1,
- accuracy < 0.1%,
- Safety factor $SF2 = \sigma_{0.2} / \sigma_{max} \geq 3$ for hand calculations and $\geq 4/3$ for Finite Element Computer Analysis,
- ambient temperature dead weight calibration at NLR
- Balance Calibration Machine (BCM) calibration at ETW.

The more general ETW requirements are provided in Reference 2 and 3.



Table 1: Aerodynamic model loads

Axial force	X	± 1500 N
Side force	Y	± 2500 N
Normal force	Z	± 18000 N
Rolling moment	L	± 600 Nm
Pitching moment	M	± 1800 Nm
Yawing moment	N	± 600 Nm
Model weight: max. 2000 N		

The major challenge was that all these requirements had to be fulfilled in cryogenic conditions and in a statically indeterminate structure. Because the TSR is a statically indeterminate structure the resultant loads in each balance are dependent on the stiffness ratios of the assembled TSR parts including the wind tunnel model. Therefore a simple Finite Element Method (FEM) model of the complete structure was made to calculate the balance loads from the known model loads, see Figure 3. This is an iterative process because the balance loads are also dependent on the balance design (stiffness).

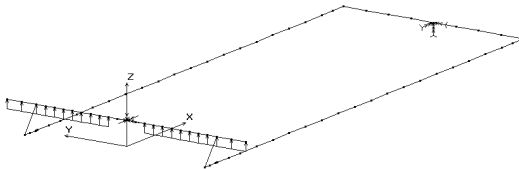


Figure 3: FEM Beam model of the TSR including loaded dummy wing

Also the balance loads themselves had to be tuned because they directly effect the high loads on the small wing-boom interface. The wind tunnel model was simulated by a representative wing. The main parameters for the tuning are the torsional stiffnesses of the booms and the balances. Finally the load range of Table 2 was determined for each balance. These loads include the static and dynamic ($\pm 20\%$) aerodynamic loads and the model weight.

Table 2: Combined loads for each TSR balance

Axial force	Fx	± 1100 N
Side force	Fy	± 1800 N
Normal force	Fz	± 13000 N
Rolling moment	Mx	± 450 Nm
Pitching moment	My	± 1300 Nm
Yawing moment	Mz	± 450 Nm

2.2 Balance design

Since the individual balance loads in the assembled TRS are known, the balances can be considered separately in the design, manufacturing and calibration process. The balances were designed following the standard NLR design procedure (Ref. 4) which consists of three major phases, see Figure 4. The design is based on a moment type balance made from one piece of material by spark erosion.

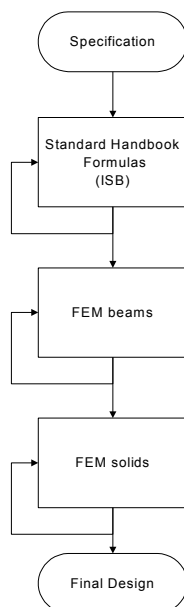


Figure 4: NLR balance design procedure

Infinite Stiff Beams (ISB)

In the seventies and eighties of the last century NLR balances were still mainly designed without the use of computers. The formulas to calculate the stresses and strains were based on standard handbook formulas for beams (tension, compression, normal bending, s-shape bending). Each design-iteration needed laborious and time-consuming calculations by hand. As soon as the maximum stress satisfied the safety factor and the output was sufficient to produce



an acceptable sensitivity, the design was ready. Extensive optimisation of the design was not possible. Once the balance was manufactured and calibrated a useful feedback was available on the validity of the design calculations. Sometimes the output of the individual strain gauges were measured during an interim calibration before the gauges were connected in Wheatstone bridges. Based on years of experience in designing and building different type and sizes of balances a factor was introduced to account for the differences between the predicted and actual stresses. It turned out that the discrepancy between predicted and actual stresses was not always the same. Therefore, the approach adopted was to design balances with beam shapes that were predictable with the standard formulas and (for the time being) not to introduce formulas for exotic beam shapes. As an example, NLR tried to avoid U-shaped cross sections of the main beams in the axial force element. In order to make the ISB phase shorter a dedicated computer program was written. With this program it was possible to calculate thousands of axial force elements within a night shift on a personal computer. The inputs for the program were the lower and upper boundaries of length, width and thickness of the flexures, and the lower and upper boundary of the number of flexures. When the configuration satisfied the upper limit for the stress and the lower limit for the axial force output the parameters of the configuration were saved. From all the solutions the most optimum was selected. In this selection process manufacturing aspects were also taken into account.

The material of the two new TSR balances is 18 Ni Maraging Steel Grade 200 with a yield strength of 1430 MPa. For the axial force bridge a Wheatstone bridge of 8 strain gauges with a gauge-factor of 2 and an excitation Voltage of 10 Volt was foreseen in order to have about 8 mV output due to the axial force. The resulting design targets for the ISB phase were:

1. Maximum stress: $1430 \text{ MPa} / 3 * 1/2.1 = 227 \text{ MPa}$
2. Minimum measuring stress: 55 MPa

The factor 1/2.1 is an empirical factor which accounts for the difference between the calculated values and the real values. This factor can be split in almost two equal contributions that represent the difference between the ISB and the FEM beam models (1.5) and between the FEM beam and the FEM Solid models (1.4).

Based on the ISB calculations an axial force element with about 6 flexures per set was chosen. The dimensions of each flexure were 20 x 14 x 2.5 mm. The measuring flexure was 10 x 8 x 2.5 mm. This configuration satisfied the maximum stress requirement although the stress level in the measuring flexure due to the axial force was somewhat low. However, this was sufficient



to start with the next phase: the model had still sufficient design freedom to optimise the design further.

FEM Beams

At the end of the eighties the first FEM models of balances were built by NLR and calculated on a main-frame computer at another institute after which the results were sent back to NLR. This was at that time also a time consuming process, however the calculated results were more accurate. As input for the first FEM model the last ISB model was used. So, the standard handbook calculations were still useful.

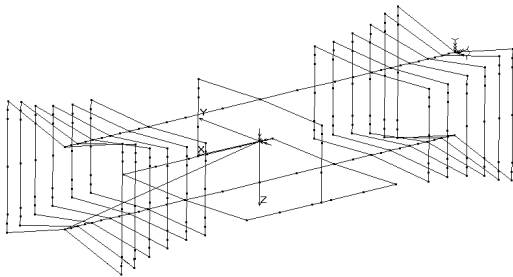


Figure 5: FEM Beam model of the axial force element

In this design phase a FEM model of beam-elements of the axial force element was made, see Figure 5. Due to the finite stiffness of the main beams the results are more realistic. More important is the difference in the trends between ISB and FEM-beams. In Figure 6 is shown that in ISB it is worthwhile to add flexures to reduce the maximum stress in the flexures, for the FEM models this is not always true, see Figure 7.

It may be interesting to see a same figure of comparable FEM solid models. However, during the design process such a figure will not be generated because it is the intention to reduce the solution space and to converge to the optimal design.

During the iterations in the FEM beam phase the properties of the main beams were not changed, only the dimensions and the number of flexures were changed. By changing the thickness and the height of the flexures it is possible to average the stress in the flexures. Pointed out in Figure 7: it is possible to reduce the maximum stress to about the average stress. The maximum stress requirement for the FEM beam phase is:

$$1430 \text{ MPa}/3 * 1/1.4 = 340 \text{ MPa}$$

This FEM beam model of 6 flexures with different dimensions satisfied this requirement and was a good starting point for the FEM Solid phase.

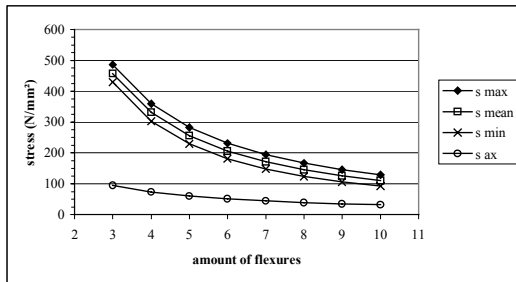


Figure 6: Stress level trends in ISB models

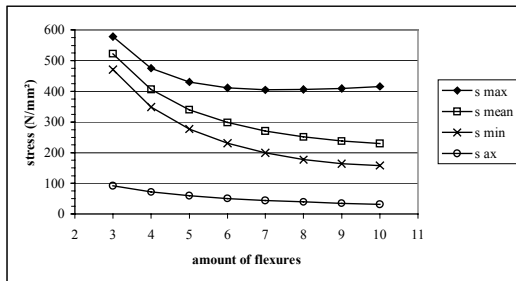


Figure 7: Stress level trends in FEM beam models

FEM Solids

Since the use of FEM Solids in the design of balances it was not longer necessary to use certain limited balance shapes in order to be able to calculate the stress levels accurately. The manufacturing possibilities, sensitivity, stiffness, interference, maximum stress etc. are the criteria for the design iterations in this phase.

Since 5 years NLR generates a FEM Solid model by using a macro containing the relevant commands of the FEM program. By using this macro it is easy to change the dimensions of the balance parts. However, within a certain macro the variations are limited. This is the reason that over the past years several different macros have been written.

The maximum stress requirement for this phase is:

$$1430 \text{ MPa}/3 = 476 \text{ MPa}$$

In Figure 8 the final FEM Solid model of the TSR balance, loaded by an axial force is shown. It appeared in this phase that it was possible to reduce the amount of flexures from 6 to 5.

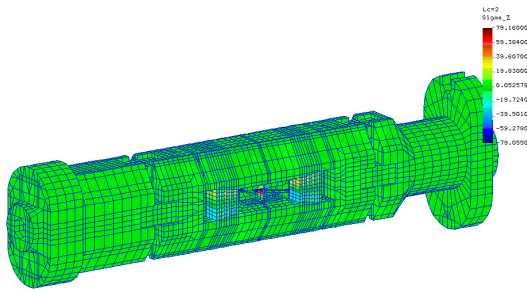


Figure 8: FEM Solid model loaded with an axial force

This FEM model is used to derive:

- the optimal locations of the strain gauges,
- the theoretical sensitivities (output),
- temperature distribution,
- thermal output,
- maximum Von Mises stress (safety factor),
- Load Rhombi equations,
- Stiffness characteristics.

The geometry of the balance is modelled with Solid 3D linear 8 nodes iso-parametric elements, 12333 Solid elements in total. All nodes from the end plane of the non-metric flange are restricted in all six degrees of freedom to simulate the clamping of this flange on the booms of the TSR. The loads are defined in the balance load centre. The loads are transferred to the metric flange by means of 180 RBARS (infinitely stiff bars) which are the modelled connections between the balance load centre and the nodes of the metric flange. For thermal calculations these RBARS are not necessary. Eight load cases were defined: load case 1 to 6 are the six load components of Table 2, load case 7 is the worst case combination of these 6 load components and load case 8 and 9 are two axial temperature gradient situations of 5 K and 30 K respectively.

Output

On each intended location of a strain gauge an element node is positioned. The stress-states of these selected nodes are easily extracted into a spreadsheet program, whether the load case is a force, moment or temperature. Following Hooke's law the corresponding strains can easily be calculated. Subsequently, by combining the results of the appropriate nodes in a Wheatstone bridge formula the resulting output can be calculated.



Table 3: Calculated output in μVolt

	M11	M2	M3	M4	M5	M6
	10 V					
$F_x = 1100 \text{ N}$	8559	0	-1	0	-1	0
$F_y = 1800 \text{ N}$	0	2865	0	7	0	-2618
$F_z = 13000 \text{ N}$	1650	0	4233	0	4574	0
$M_x = 450 \text{ Nm}$	0	-38	0	4301	0	67
$M_y = 1300 \text{ Nm}$	-167	0	-4297	0	4543	0
$M_z = 450 \text{ Nm}$	0	7075	0	-442	0	6215

The calculated output of Table 3, together with the single loads of the specified nominal load range, can be used to determine a 6x6 linear theoretical calibration matrix. The inverted matrix gives the linear data reduction matrix and can be used to perform a theoretical accuracy analysis.

Assume a reading vector:

$$(M11, M2, M3, M4, M5, M6) = (5, 2, 2, 2, 2, 2) \mu\text{Volt}$$

with an assumed error per strain gauge bridge. The absolute data reduction matrix times the error vector gives the calculated worst case errors in N and Nm :

$$(F_x, F_y, F_z, M_x, M_y, M_z)_{\text{error}} = (0.7, 1.3, 5.9, 0.2, 0.6, 0.1) \text{ N or Nm.}$$

These errors can also be given as percentage of the nominal load range.

$$(F_x, F_y, F_z, M_x, M_y, M_z)_{\text{error}} = (0.07, 0.07, 0.05, 0.05, 0.05, 0.03) \%$$

Maximum Von Mises stress (safety factor),

The maximum Von Mises stress in the balance due to the nominal loading in a worst case combination is $\sigma_{\text{max Von Mises}} = 507 \text{ N/mm}^2$. This maximum stress is located in the moment section on the model side for the load combination $+f_x, +f_y, +f_z, +M_x, +M_y, -M_z$. This combination was found by checking all the $2^6 = 64$ combinations of the load components of Table 2. In fact, due to the symmetry of the balance (port/starboard, up-/downstream) only 16 combinations had to be checked. The maximum stress resulted in a safety factor of 2.8 on yield. Although the maximum stress is higher than the design target of 476 MPa, the corresponding safety factor is rather large compared to the safety factor for FEM calculations as given in chapter 2.1.



However, by following this approach ETW allowed NLR to omit further fracture mechanics, crack growth rates or fatigue life analysis.

Stiffness characteristics

The translations and rotations of the FEM model nodes of the metric interface plane (load introduction) are given relative to the non-metric interface plane (clamped). These translations and rotations can be used to calculate the displacement of the adapter relative to the balance at the down stream end of the balance: 1.68 mm in Z-direction and 0.92 mm in Y-direction. The translations and rotations of these nodes can also be transformed into theoretical deflection coefficients of the balance using the nominal loads.

Load Rhombi equations

Besides the nominal loads of Table 2 the load envelope of the balance is limited by Load Rhombi equations. In fact the Load Rhombi formulas are stress-monitoring equations and can also be used as such. In the final FEM Solid model several critical areas were selected: main beams, moment sections, axial force measuring flexures, horizontal de-coupling flexures and vertical de-coupling flexures. The considerations for the interfaces were somewhat different and not based on the FEM model. In the set load rhombi equations at least one equation should cover the critical interface. The main stress components of the 6 load components of the nodes in the critical areas are added absolutely. (The main stress component for the beam, moment sections and the horizontal de-coupling flexure is σ_x , for the axial force measuring flexure and the vertical de-coupling flexures the main stress component is σ_z).

Example Node1:

$$\sigma_{\max 1} = |\sigma_x|_{fx} + |\sigma_x|_{fy} + |\sigma_x|_{fz} + |\sigma_x|_{Mx} + |\sigma_x|_{My} + |\sigma_x|_{Mz}$$

From each critical area the most critical node is selected. The contribution of each load component in the stress summation is divided by the load component used in the FEM calculations. This gives the load rhombi coefficients.

Example Node 1:

$$\begin{aligned} c11 &:= |\sigma_x|_{fx} / fx & c14 &:= |\sigma_x|_{Mx} / Mx \\ c12 &:= |\sigma_x|_{fy} / fy & c15 &:= |\sigma_x|_{My} / My \\ c13 &:= |\sigma_x|_{fz} / fz & c16 &:= |\sigma_x|_{Mz} / Mz \end{aligned}$$

The load rhombi coefficients are used in the following load rhombi or load monitoring equation:

$$c11|fx|_{\text{actual}} + c12|fy|_{\text{actual}} + c13|fz|_{\text{actual}} + c14|Mx|_{\text{actual}} + c15|My|_{\text{actual}} + c16|Mz|_{\text{actual}} = \sigma_1 \leq 476 \text{ MPa}$$



Normally the load equation criteria are the same as the design objectives. For each load component at least one equation must be limiting. For the TSR balances 8 equations are sufficient to monitor the complete balance. Two of these equations represent the interfaces and monitor the bolt loads and separation of the interface planes.

Before a wind tunnel test these equations can be used to determine whether a balance is suitable for the test. During the wind tunnel test the equations can be used online to check for overload. The equations are only to monitor or to limit the stresses in the balances from a mechanical point of view, no measuring criteria are used (interpolating or extrapolating calibration data, maximum input voltage Data Acquisition system etc.)

Temperature effects

The thermal stresses were calculated for two different situations:

- an axial temperature gradient of 10 °C over the complete balance,
- an axial temperature gradient of 60 °C over the complete balance.

These situations simulate respectively the specified gradients of 5 and 30 K over the measuring part of the balance (Reference 2).

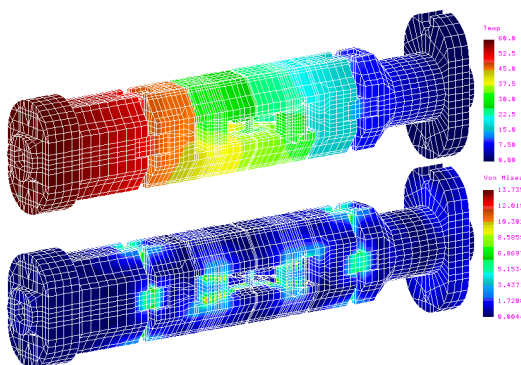


Figure 9: Temperature distribution and corresponding Von Mises stress due to a temperature gradient of 30 K over the measuring section of the balance.

The calculation of the temperature effects is performed in two steps. First the steady state temperature distribution in the balance is calculated based on specified temperature levels of the interface planes (boundary condition). The nodal temperatures are stored for use in the next step. Second, the stresses are calculated based on the nodal temperatures. From Figure 9 it is clear that the thermal stresses are negligible from a mechanical point of view. However, the gradient of 5 K produces a theoretical output of about 2 μ Volt on the axial force bridge.



2.3 Additional parts

In parallel with the development of the TSR balances ETW also developed small diameter heated packages enclosing high precision QFlex inclinometers. These would be attached to the forward side of the balance adaptors as close as possible to the forward side of the balance. The accurate measurement of incidence over the complete range of test conditions was a prerequisite for the accurate determination of the force vectors generated by the model. NLR allowed adequate space into the nose fairing designs to enable a heated package with 50 mm diameter to be installed. Figure 10 shows the forward nose fairings together with the new heated package developed by ETW for this application.



Figure 10: Forward nose fairings and ETW's QFlex heated package

3 Manufacturing

The balances were manufactured using standard workshop techniques including spark erosion. A picture of one TSR balance is provided in Figure 11. The instrumentation materials (gauges, bonding, coating, etc.) and procedures are more or less standard for cryogenic balances. A test-beam of the same material batch as the balances and instrumented with the same instrumentation proved to be very useful in combination with a mathematical model of the beam temperature characteristics. The test beam delivered the parameters for the mathematical model and subsequently the mathematical model delivered the values of the resistors to compensate for the sensitivity and zero shift. The balances are each provided with six Pt100 RTD temperature sensors spread over the balance.

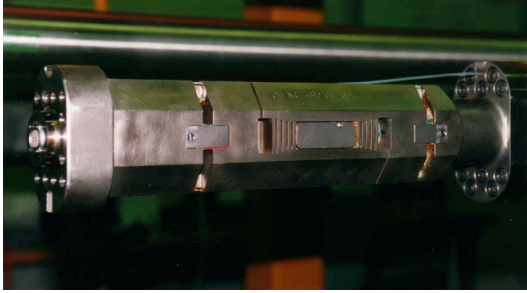


Figure 11: *TSR boom balance*

4 Checks

After manufacturing and instrumentation the individual balances were checked at NLR, and later under better-controlled conditions also at ETW. The following checks were performed:

- Zero shift,
- Sensitivity shift,
- Pressure effects,
- Moisture checks and insulation resistance,
- Creep.

5 Calibration Activities

5.1 Ambient dead weight loading calibration at NLR

For the initial dead weight calibration at NLR a new calibration model was designed. In combination with a dummy wing this model can also be used to load a dummy wing mounted on the TSR. A picture of the calibration model is provided in Figure 12. The central part of the calibration equipment is intended to ensure a load transfer on the balance, which is comparable with the load transfer of the adaptors of the TSR.



Figure 12: Normal force check loading using 200 Kg precision weight pile

High stiffness is required to make sure that only the balance will deform under external loading. The loads for the calibration of f_z are applied by means of an elastic hinge mounted on the central part. The front side of the balance support and the four sides of the central parts are suitable places for levelling instruments. For the calibration of the moments four arms of 0.5 m are mounted on the central calibration part. The arms are intended to apply moments due to small (parasitic) forces. Elastic hinges are the connections between the calibration model and the weight suspension equipment. By using these hinges virtually pure forces will be exerted on the calibration equipment and undesired parasitic moments due to shift of the force-line of action will be reduced. This shift could be caused by the deformation of the calibration equipment or limited levelling possibilities (accuracy of levelling instruments!). By making the calibration parts as stiff as possible and by using high accuracy levelling instruments these parasitic moments can be mostly avoided.

5.2 Calibration at ETW in the Balance Calibration Machine

Following delivery of the balances and the associated loading equipment to ETW the first step in the calibration activity was to install one of the TSR balances in the Balance Calibration Machine (BCM). A detailed description of the BCM is provided in Reference 2 and the associated quality of results obtained from typical calibrations is provided in Reference 5; an overall view is provided in Figure 13.



Figure 13: The ETW balance calibration machine



Figure 14: TSR balance installed in BCM

The installation of the balances in the BCM required the use of intermediate adaptors. One front adaptor and one rear adaptor, together with all additional loading equipment, were supplied by NLR. The adaptors are compatible with the large Vascomax C-200 rings of the BCM. Figure 14 shows a detailed view of one of the TSR balances installed in the BCM. From this figure it can be seen that the balance is supported from two adaptors with each adaptor having a flange joint connection to the loading and measuring sides of the BCM. It can also be seen from this figure that the adaptors and the balance are installed within a small cryogenic chamber to enable discrete temperature levels to be set. For this first calibration of the TSR balances each balance was calibrated at 12 different temperatures in the range 325 to 115 K. This covered the complete range of temperatures defined in the initial balance specification. In practice this range adequately covered the anticipated range of conditions to be tested in the subsequent wind tunnel tests. The calibration results demonstrated that accuracy achieved by each balance was within the overall specification, i.e. each single load component was within 0.1%.

From the BCM calibration matrices it was also possible to derive the balance zero readings and the main sensitivity for each component at each discrete calibration temperature. An example of the effective zero drift (converted into N) and the sensitivity are provided in Figures 15 and 16



respectively for the axial force component. The zero drift is seen to vary in opposite directions for each TSR balance with a maximum variation of around 0.1 N/K for the right balance and 0.05 N/K for the left balance. The variation of sensitivity with temperature shows that the balances are matched over the complete temperature range within 2% with each balance showing an individual sensitivity variation of around 0.5%. From this brief review of typical results it is clear that although the balances are relatively insensitive to temperature it is still necessary to calibrate at discrete temperature steps to achieve the required accuracy.

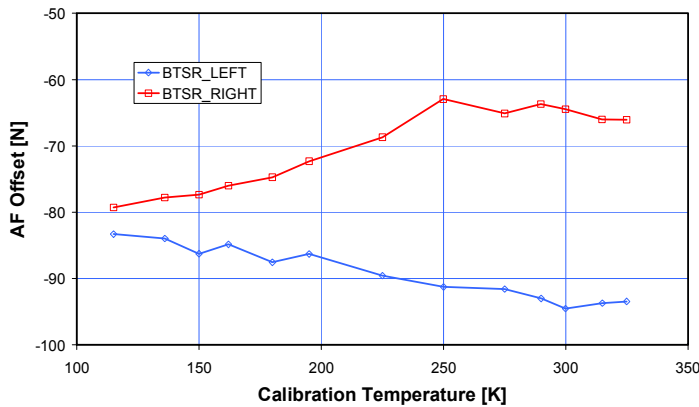


Figure 15: Axial force offsets obtained from calibration in ETW's BCM

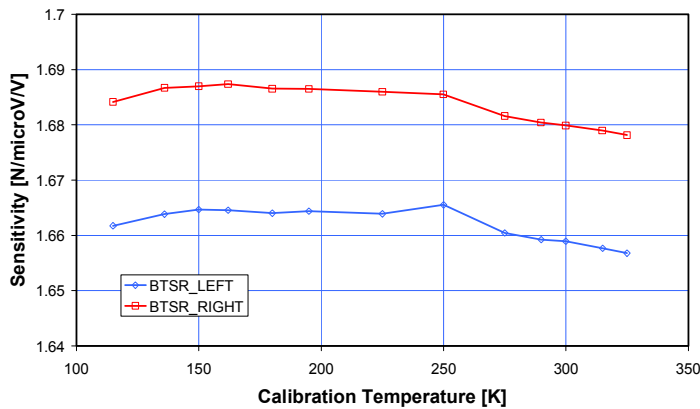


Figure 16: Axial force sensitivity obtained from calibration in ETW's BCM



Figure 17: Normal force check loading using 2 x 500 Kg certified weights

5.3 Check Loadings on Individual Balances

In line with current best practices at ETW each balance was subjected to a check loading to validate the balance matrices obtained from the BCM at ambient temperature conditions. These trials do not form a part of the overall calibration but simply provide an independent loading method. Using this philosophy it is possible to achieve high levels of confidence in the calibration over a range of conditions. The individual check loadings were primarily aimed at validating the calibration matrices with particular emphasis on the axial force, normal force and pitching moment components. The interaction of normal force and axial force components was also checked using this method. Figure 12 shows the typical set-up for a normal force loading using a 200 Kg precision weight pile. This figure also shows the calibration body previously used during the calibrations at NLR, which is used to load each balance individually. Figure 17 shows the method used to apply higher normal force loads, in this case the balance has been loaded with 2 certified 500 kg weights supported on a loading frame connected to the calibration adaptor via chain links. Although this loading method may appear rather crude, experience has shown this method to be an effective means to validate the balance normal force / axial force alignment and, in general, the applied loads are known to high accuracy.



5.4 Connected Balance Check Loadings

In the final application both twin boom balances are used to determine the overall loads generated by the model. To assess the calibration philosophy for the connected balances a dummy wing was used to connect each balance installed on the Twin Sting Rig and this, in turn, was used to load the complete mechanical set-up from the model interface to the Model Cart structure.



Figure 18: Loading the TSR test assembly from the VTCR basement

An integral balance adaptor / nose boom fairing was installed on each balance and the dummy wing was then installed using the standard model interface joints. The complete assembly was then installed in one of ETW's Variable Temperature Check-out Rooms (VTCR). The complete TSR assembly was then loaded using dead weights over a range of temperatures and loading conditions compatible with the individual balance specification. Certified calibration weights were again used for this application and Figure 18 shows the loads being applied in the basement area located below the VTCR. A view of the TSR installed in the VTCR with the dummy wing installed is provided in Figure 19. In this figure an Inconel loading rod is attached on one end to the dummy wing and on the other end to the loading frame shown in Figure 18. A small hole cut into the VTCR floor enabled the loading to be made without any fouling. Using this method the TSR assembly was loaded with the certified weights up to 20 kN with the TSR both upright (Roll = 0°) and inverted (Roll = 180°). The VTCR enabled loadings to be applied at discrete temperatures compatible with the conditions planned for the subsequent wind tunnel test series. The balance residuals (actual load – loads measured by each balance) obtained from these loading trials are shown in Figures 20 and 21 for normal forces and axial force respectively.



Figure 19: TSR with dummy connecting wing installed in the VTCR

The results from these trials demonstrate that the combined output from the new boom balances closely match the applied loads over a range of test temperatures. The scatter seen in the data is primarily due to small oscillations in the applied dead weights with axial force being particularly sensitive. The main result from these trials was that the forces and moments measured by the individual balances could be summed without the need for any additional adjustments. This result was very significant in that the calibration effort for future applications could be restricted to the individual balances and, providing that the interface joint with the model components was similar, no additional model related calibration efforts would be required.

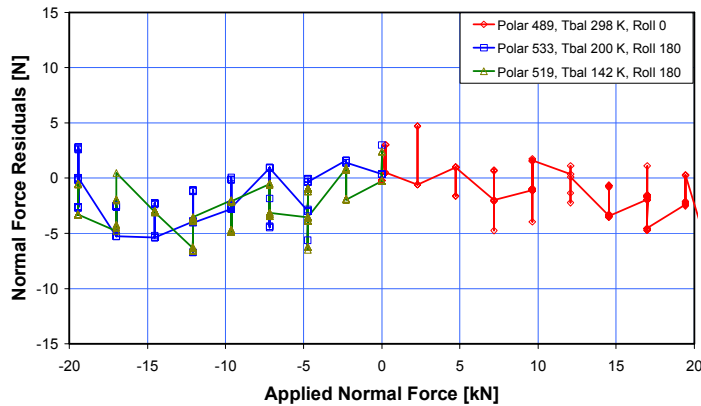


Figure 20: Normal force residuals from connected balance check-loadings

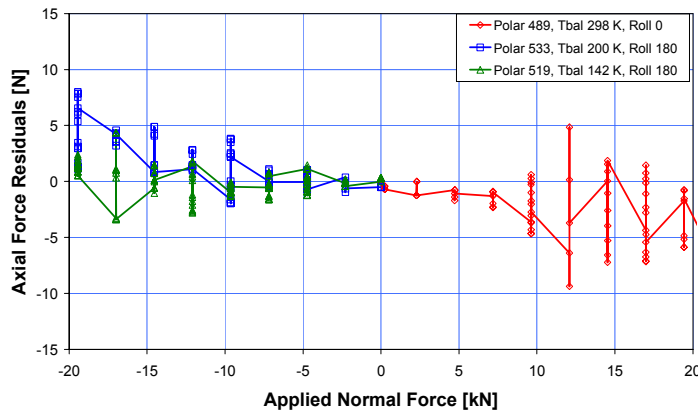


Figure 21: Axial force residuals from connected balance check-loadings

6 Twin Sting Rig Wind Tunnel Test Results

Following the successful calibration and check loading activities the model was installed onto the new twin boom balances. A general view of the finished model supported from the TSR is provided in Figure 1. From this figure it can be seen that the dummy sting was installed for this phase of the test programme and a similar configuration without dummy sting, and with the rear fuselage completed, was also tested.

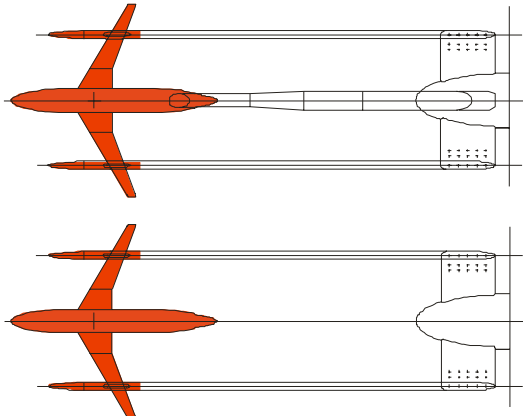


Figure 22: Determination of sting corrections using twin boom balances

A schematic representation of these two configurations is given in Figure 22. During this test phase the model was tested over a range of temperatures from 300 K down to 115 K and at pressure levels from approximately 112 - 345 kPa. At Mach numbers around the cruise condition this resulted in Reynolds numbers in the range 4-42 million. In terms of the balance load ranges the maximum normal force achieved during this first TSR test series with the new balances was around 20 kN or very close to the balance limits defined in the overall balance specification.

Throughout the test series, prior to and following each block of test polars, it was normal practice to record zero data and undertake no-wind traverses upright and inverted. These wind-off checks are considered to form an essential part of the check procedures at ETW and provide a valuable indication of the balance zero drift and overall repeatability. The balance residuals after subtraction of the model weight terms give an indication of the data quality. Figure 23 shows the axial force, normal force, and pitching moment residuals over a range of test temperatures. These residuals have been derived from the ETSR boom balances with each balance utilising its own calibration matrix. These small residuals show that the balances are measuring the model weight to high accuracy over a range of conditions. What is not shown in this figure is that the individual boom balances do not necessarily provide identical outputs, whilst the overall summing of the twin balances is extremely accurate. This feature is associated with the ability of the twin balances to measure the overall stresses in the complete system as would be expected with a mechanical assembly utilising mechanical joints of adequate quality.

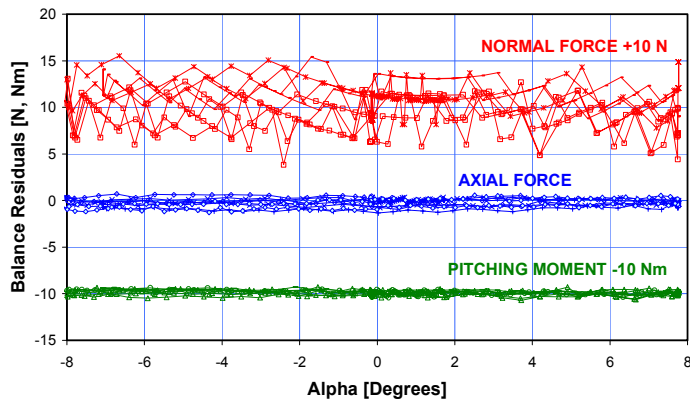


Figure 23: Axial force, normal force, and pitching moment residuals obtained from no-wind polars

Throughout the wind-on part of the test series several repeat polars were undertaken to assess the test technique and establish the level of short-term repeatability. Figures 24 and 25 provide a comparison of three polars acquired at high speed at a Reynolds number of 32 million. The three repeat polars were acquired using both the continuous traverse technique and the pitch & pause technique. The lift and drag characteristics are shown to have adequate repeatability. In line with the overall balance specification the objective of achieving similar levels of repeatability to a single sting / single balance model has been achieved.

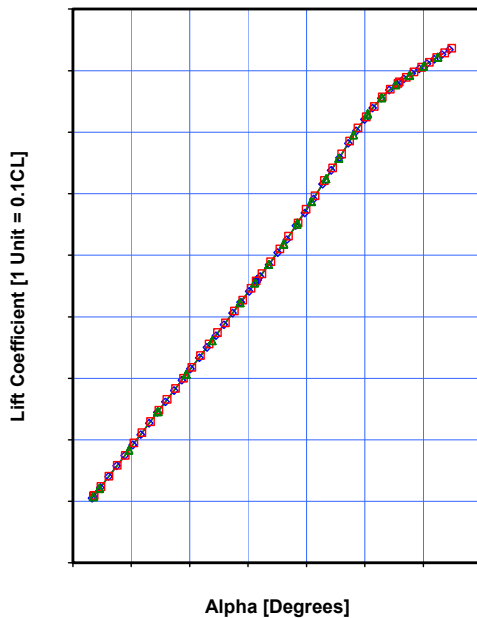


Figure 24: Lift repeatability at high Reynolds number

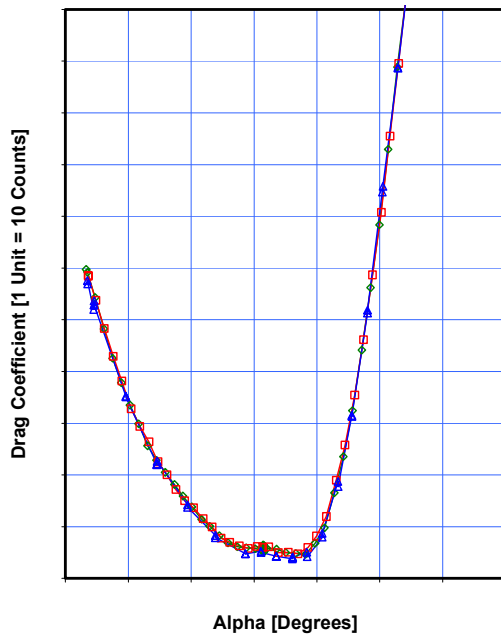


Figure 25: Drag repeatability at high Reynolds number

In the context of sting corrections the quality of the test results is better gauged by the difference between two test configurations. An example of the drag increment repeatability is provided in Figures 26 and 27 for both low and high Reynolds number conditions. These drag increments represent the difference between a configuration with a distorted afterbody / sting cavity / dummy sting representation and a configuration with a full afterbody representation without a dummy sting. The repeatability is demonstrated by differencing all combinations of repeat continuous polars at the selected test conditions. From these figures it can be seen that the general level of uncertainty demonstrated by this new technique is better than 1 drag count irrespective of Reynolds number. These low levels of uncertainty demonstrated within the sting interference part of the HiReTT programme are considered to be an excellent starting point for this new twin sting test technique.

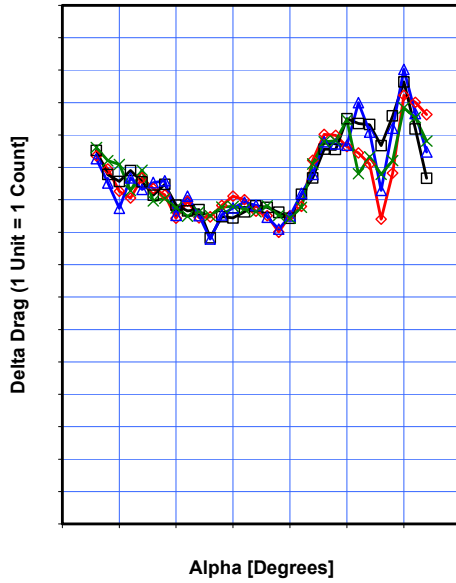


Figure 26: Increment drag repeatability at low Reynolds number

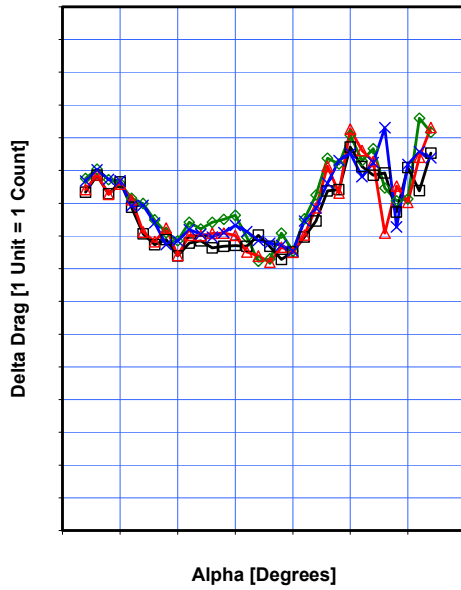


Figure 27: Increment drag repeatability at high Reynolds number



7 Conclusions

Close co-operation between ETW and NLR has successfully lead to the design and manufacturing of a Twin Sting Rig including two state of the art cryogenic balances. The Finite Element Method proved to be essential in the design-process of the Twin Sting Rig and the balances. With the Enhanced Twin Sting Test techniques ETW has a state of the art test technique for cryogenic sting interference investigations.

8 References

- [1] D. Schimanski, J. Quest
Tools and techniques for high Reynolds
number testing status and recent
improvements at ETW
AIAA 2003-0755
- [2] U. Walter
ETW User Guide, Revision A
Document ETW/D/95001/A
January 2004
- [3] D. Schimanski, T. Vohy
ETW Model Design Handbook, Revision A
Document ETW/D/95001/A
July 1999
- [4] Vos, H.B.
Strain Gauge Development at NLR
First International Symposium on Strain
Gauge Balances
October 1996
- [5] Dr.-Ing. Ulrich Jansen
Automatic Balance Cryogenic Calibrations at ETW – Pushing the Limits
Third International Symposium on Strain Gauge Balances
Darmstadt, Germany, May 2002